Sys Rev Pharm 2020;11(10):749-761
A multifaceted review journal in the field of pharmacy

The Effort to Lower Titanium Oxidation in the Sintering Process of Titanium Alloy: A Review

Fitria Hidayanti[1*], Sugeng Supriadi[2], Bambang Suharno[3]

[1,3]Metallurgy & Material Engineering, Faculty of Engineering, Universitas Indonesia, Depok, 16424, Indonesia
[2]Mechanical Engineering, Faculty of Engineering, Universitas Indonesia, Depok, 16424, Indonesia

Corresponding Author: Fitria Hidayanti
Email: fitriahidayanti@gmail.com

ABSTRACT

Titanium alloy Ti-6Al-4V has a combination of mechanical properties for implants such as good ductility, high resistance to corrosion, and good biocompatibility. However, the use of this alloy is limited due to low oxidation resistance at high temperatures from the Metal Injection Molding (MIM) sintering process where oxygen reacts with titanium forming TiO_2. The formation of TiO_2 gave a negative influence in terms of lowering the ductility so as to make the material fragile (embrittlement). In addition, TiO_2 will form pores on the implant and reduce the density of Ti-6Al-4v. Some researchers sought to reduce the formation of TiO_2 in several ways, including the reactive oxygen scavenger of rare earth (RE) and the oxygen-stabilized compounds and the control and arrangement of sintering atmospheres. In addition, the use of the new sintering method Arc Plasma Sintering (APS) gives refinement on the surface of sintering results and the short sintering time of APS can minimize the occurrence of oxidation reactions. Unfortunately, there has not been any research that gives a new method on the MIM process to minimize the formation of TiO_2. Therefore, this paper aims to review new methods in the MIM process by adding oxygen scavenger from rare earth which is reactive based on Gibbs free energy diagram of standard oxide formation so that the elements and compounds can form the rare earth oxide with a brief variety of sintering time using APS in a controlled argon atmosphere. This new method is expected to provide a solution to reduce the formation of TiO_2 in Ti-6Al-4V alloy so that the required mechanical properties as a condition of implant material can be maintained.

Keywords: Metal injection molding, TiO_2, oxygen scavengers, argon, Arc Plasma Sintering

Correspondence:
Fitria Hidayanti
Metallurgy & Material Engineering, Faculty of Engineering, Universitas Indonesia, Depok, 16424, Indonesia
Email: fitriahidayanti@gmail.com

INTRODUCTION

According to Indonesian Agency Central Statistical data in 2017, the number of injuries reached 103.2 thousand cases. Data shows that the growth of accidents per year reaches 0.77%. The number of road accidents has fluctuated over the last 10 years, the highest increase occurred in 2012, i.e. 117.9 thousand cases, but in 2010 only happened 66.5 thousand cases. The number of patients with severe injuries ranged from 20-40 thousand incidents and 50% of them have broken bones. The case of fractures causes the bones to be crushed or broken into parts so that some require a miniplate in surgery/bone surgery. Mini plates used in surgical/bone surgery were imported from some countries such as Switzerland, China, India, Turkey, Germany, and the United States of America with prices ranging from the US $20 – 40 per miniplate. Meanwhile, the surgery at least needs about 30 mini plates for a leg operation.

The material used as an implant, generally titanium alloy, widely used as an ingredient for bone surgery requiring mechanical strength, osteosynthesis, and high biocompatibility.[1] According to Ratner[2], The Ti-6Al-4V alloy is treated as to be biocompatible with the human body. Biocompatibility is the material's ability to perform its function in patients for specific applications, and biomaterials are natural or synthetic substances that are temporarily or permanently accepted in the human body.[3] The process used in the manufacture of mini plates for implants is Metal Injection Moulding (MIM). MIM is a good technique for the production of components for stainless steel, titanium, and other metals. Over the last decade, the method has also attracted attention as a promising technique for the manufacture of complex titanium components for a wide range of applications in the biomedical, aerospace, automotive, and other industries. Historically, the need to use a finely rounded titanium powder (0.45 µm) with a low titanium dioxide content has hindered the MIM titanium industrial application from an economic perspective.[4]

The addition of oxygen scavenger element of rare earth metal is done to improve reaction with oxygen, such as lanthanum (La)[5], cerium (Ce)[6-8], neodymium (Nd), gadolinium (Gd)[9] and yttrium (Y)[10]. Research showed that the ability to scavenge oxygen of the rare earth (RE) element in the series Y (yttrium) > Er (erbium) > Dy (dysprosium) > Tb (terbium) > Gd (gadolinium)[11,12] (based on Gibbs free energy). The high yttrium potency of titanium alloys in oxygen scavenging where the distributed Y_2O_3 dispersoid is evenly produced from added by the 0.1 wt.% Y in titanium alloys containing only 0.07 wt.% oxygen[13]. Hidalgo and Limberg[14] stated that the addition of a small amount of 0.5 wt.% yttrium to Ti-6Al-4V which MIM processed to lead to colony refinement in situ Y_2O_3 formed during sintering, resulting in increased fatigue strength observed. According to Yan[15], yttrium hydride (YH_2) is seen to have more advantages than any other form of RE-based material because it releases hydrogen. Hydrogen is capable of reacting with oxide surface and produce a clean surface. It is also known that the activity around Ti particles is enhanced by the presence of H_2 and contributes to better densification. But in research using, yttrium hydride has not discussed the effect of changing the mechanical properties of its alloys on the formation of Ti-6Al-4V-YH_2 composite. Yan[16] indicated that the transmission electron microscopy (TEM) analysis with the addition of a small amount of

yttrium hydride in the alloy powder metallurgy resulting in a yttrium oxide formation. Yttrium is potentially in scavenging oxygen. In addition, the β-Ti phase is free from the α-Ti phase of the nanoscale by yttrium. As already known, Yu[17] stated that there were 48 slips of the system per cell from β-Ti while there were only 3 slips of system per cell of α-Ti. This is the reason why β-Ti has high ductility. Therefore, according to Yan[16], this change of microstructure contributed to an increase in ductility (~ 90%).

In addition to RE-based material, according to Yan and Tang[13], the addition of oxygen scavenger from the compounds that stabilized oxygenated such as Ti_2C and $Ti_4Fe_2O_x$ can be done. The formation of Ti_2C is associated with oxygen and forms Ti_2C oxygen stabilizer. Due to local concentrations of oxygen, a form of oxygen-sensitive stages, for example, α-grain, ω and/or α_2 limits can be avoided. However, the solubility of oxygen in Ti_2C is generally below 10 wt.% O, indicating that oxygen-scavenging capability is Ti_2C less than RE-based material such as YH_2, leading to the creation of Y_2O_3 contains up to 60 wt.% O. Controversy still exists because the Ti_2C contains more oxygen than the Ti matrix. The second type of oxygen stabilized compound is a group of intermetallics such as $Ti_4Fe_2O_x$ that are formed by the presence of TiFe even with oxygen concentration in the trace level (approximately 0.1 at% ≈ 0.03 wt.%). In other words, research from the $Ti_4Fe_2O_x$ phase expects that this intermetallic phase can perform oxygen scavenging from PM Ti. However, the mechanism is unclear despite the fact that the overall oxygen scavenging is expected to exceed the compound's efficiency Ti_2C.

Control and arrangement of the atmosphere of sintering also performed M. Jabir[18] to minimize the formation of TiO_2 by reducing oxygen in the atmosphere using argon or vacuum gas. A vacuum-sintered polyethylene/Palm Stearin binder sample produces a density of 3.943 g/cm^3 and a tensile strength of 325.976 MPa. While if it is sintered with argon gas, there is a decrease in atmospheric oxygen that increases density by 11% to 4.375 g/cm^3 and increased tensile strength of 207% to 1000.1 MPa. For porosity, if sintered with argon gas, there is a decrease in atmospheric oxygen, which lowers the porosity by 78% compared with vacuum sintering[18]. Similarly, the sample with a vacuum-sintered polyethylene/paraffin Wax/Stearic Acid binder generates a density of 4.341 g/cm^3 and a tensile strength of 494.079 MPa. Meanwhile, if it is sintered with argon gas, there is a decrease in atmospheric oxygen that increases density by 0.4% to 4.359 g/cm^3 and increased tensile strength 90.4% to 940.823 MPa. For porosity, if sintered with argon gas, there is a decrease in atmospheric oxygen, resulting in decreased porosity up to 11.3% and elongation increased by 143% compared with vacuum sintering.[18]

Nevertheless, the study utilizes the oxygen scavenger's deactivation of rare earth to scavenging oxygen from a titanium alloy matrix, coupled with the argon gas flow in the control and arrangement of the sintering to reduce atmospheric oxygen, using APS as sintering mode with short sintering time to minimize oxidation, researchers have not conducted. For that, the research needs to be done by adding oxygen scavenger from rare earth in alloy Ti-6Al-4V as an implant material, combined with the use of argon gas flow in sintering process with APS mode that aims to minimise the reaction between oxygen and titanium that make up the TiO_2 layer so that the mechanical properties of the product are maximized.

LITERATURE REVIEW

Several studies were conducted to reduce the formation of TiO_2.

Uses of Rare Earth-based Oxygen Scavenger

The addition of oxygen scavenger element of rare earth metal is also done to improve reaction with oxygen, such as lanthanum (La)[5], cerium (Ce)[6-8], neodymium (Nd), gadolinium (Gd)[9] and yttrium (Y)[10, 19]. Titanium solid solution has a strong chemical affinity to scavenge oxygen. The use of a scavenger-based Rare Earth (RE) element is the most practical option. A number of titanium alloys were introduced to the RE element using rapid solidification processing (RSP). According to Leyens and Peters[20, 21], rapid reaction rate among rare earth and oxygen because oxygen is a fast spreader in the Ti molecule (at 1300 °C about ~10^{-9} m^2/s). The goal is to form a good RE oxide.

There has been an increase in the last two decades in using RE-based materials to reduce oxygen loss influence on ductility as in some of the following studies.[13]

a. A range of RE-based materials has proven effective in the oxygen scavenging of titanium solid solutions including the RE metal (such as Er and Ce)[22, 23], RE oxide with less oxygen (i.e. Y_2O_3)[24], RE hydride (such as YH_2)[16], RE boride (like LaB_6)[25], RE-silicide (such as $CeSi_2$)[26] and alloys containing RE (such as $NdAl_2$ and NdAl)[27].
b. The ability of rare earth elements in oxygen scavenging according to the following sequence Y > Er > Dy> Tb > Gd[11,12] (based on Gibbs free energy). Yttrium shows high potential in oxygen scavenging of titanium alloys. This is shown in Figure 1[13] where evenly distributed Y_2O_3 dispersoids result containing only 0.07 wt.% oxygen from adding 0.1 wt.% Y to titanium alloys.

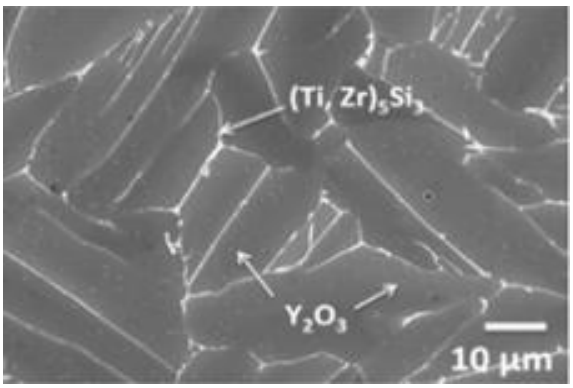

Figure 1. Precipitation dispersoid a good Y_2O_3[13]

c. RE oxides have insignificant oxygen-scavenging effects if RE oxides have very little oxygen[24]. The added pure metal RE proved to be a problem too because it should be in the form of RE oxide. The addition of the RE element in the form of a master alloy, boride, or hydride is preferred.
d. Oxygen scavenging costs should be considered. Y, Ce, La, and Sm are relatively cheap RE-metallic elements, including RE master alloys.
e. Compared to other RE-based content formulations, RE hydride (like YH_2) is seen to have more advantages because it releases hydrogen.[15] Hydrogen can respond with the oxide surface area and produce a clean surface. In the same way, the use of TiH_2 as a scratch

powder material. Furthermore, H_2 also increases activeness around Ti particles and densification becomes better.

f. When 0.3–0.6 wt% RE is used, the ductility of as-sintered Ti is successfully increased to 60–90%[16, 26]

Yttrium

Yttrium addition 0.5 wt.% (oxygen content in yttrium around 0.9%) produces a grain size that is better than 150 µm to 50 µm in the presence of Y_2O_3 forming blocking grain growth. In connection with an oxygen scavenger, the oxygen from titanium leads to a decreased tensile strength of about 70 MPa, but the fatigue force increased from 15 MPa to 60 MPa due to refinement as a result of decreased strength (Yield Strength). To understand the mechanism of formation of Y_2O_3 done XRD in-situ with synchrotron radiation. The formation of Y_2O_3 occurs at 850-1050 ^{0}C.

Hidalgo and Limberg[14] stated that the addition of a small amount of 0.5 wt.% Yttrium on Ti-6Al-4V which MIM processed to lead to colony refinement in situ Y_2O_3 formed during sintering, resulting in increased fatigue strength observed. Yttrium addition to the Ti-6Al-4V that MIM's processing leads to higher porosity, partially filled with large Y_2O_3 particles. It can be prevented by using pre-alloy master batch powders with higher yttrium content such as Ti-6Al-4V-3Y instead of pure yttrium powder. Finally, it can be proved that microstructures such as colony size of lamellar thickness have a high impact on the phatic resistance of the α/β titanium alloy for MIM. Therefore, the appropriate design of the microstructure will contribute positively to the fatigue resistance of the PM titanium alloy.

Limberg and Ebel[19], the addition of 0.1 – 0.2 wt.% yttrium in the MIM process gives the following results.

a. Refinement of the colony size increased residual porosity with the formation of several larger Y_2O_3 pores and did not increase the oxygen concentration for added by the 0.2 wt.% Y at Ti-6Al-4V.
b. It does not affect ductility for added by the 0.2 wt.% Y in Ti-6Al-4V, which is disinterring at 1400 °C.
c. The Ti-6Al-4V disinterring at a temperature of 1400 °C indicates a significant reduction in Ultimate Tensile Strength (UTS) and Yield Strength (YS) with the addition of 0.2 wt.-% Y, which cannot be reduced only by the increase in residual porosity.
d. Yttrium visible can-do oxygen scavenging from titanium.
e. There is no difference in total oxygen content between specimens with or without yttrium which suggests that it was actually scavenging oxygen out of the titanium matrix with yttrium occurring during Ti-6Al-4V sintering with yttrium.

Yttrium Oxide (Ytria)

Ramaswamy et al.[28] stated that the preparation of Ti-6Al-4V-Y_2O_3 composites with powder metallurgy was carried out using Y_2O_3 size 40 nm. For the composite itself, an additional Yttria of 1-3 wt.% was added. The highest density is obtained by adding 2 wt.% Yttria. The higher the sintering temperature, the density also increased so that the researchers obtained the highest density at the addition of 2 wt.% Yttria at a sintering temperature of 1400 ^{0}C at 87.69%.

Yttrium Hydride

Yan and Liu[15] state that the YH_2 decomposition in Ti-6Al-4V or CP-Ti is generally completeness when it reaches 1300 ^{0}C. The element Y is very responding to 1300 ^{0}C, Y will react with oxygen because Gibbs Free Energy is very negative for the formation of Y_2O_3 at 1300 ^{0}C (1440 kJ/mol). In research using YH_2, Yan and Liu[16] also studied the TEM study in detail from the as-sintered microstructure of Ti-2.25Mo-1.5Fe alloys with and without 0.6 wt.% YH_2. Some of the results include the identification of some form of Y-O oxide with little oxygen and phase homogenization associated with oxygen reduction. There are two ways to prepare TEM samples, namely twin-jet polishing (with a perchloric acid solution at -30 ^{0}C) and focused ion beam on XT Nova Nanolab 200. In TEM analysis, the crystal structure is determined using selected-area electron diffraction (SAED).

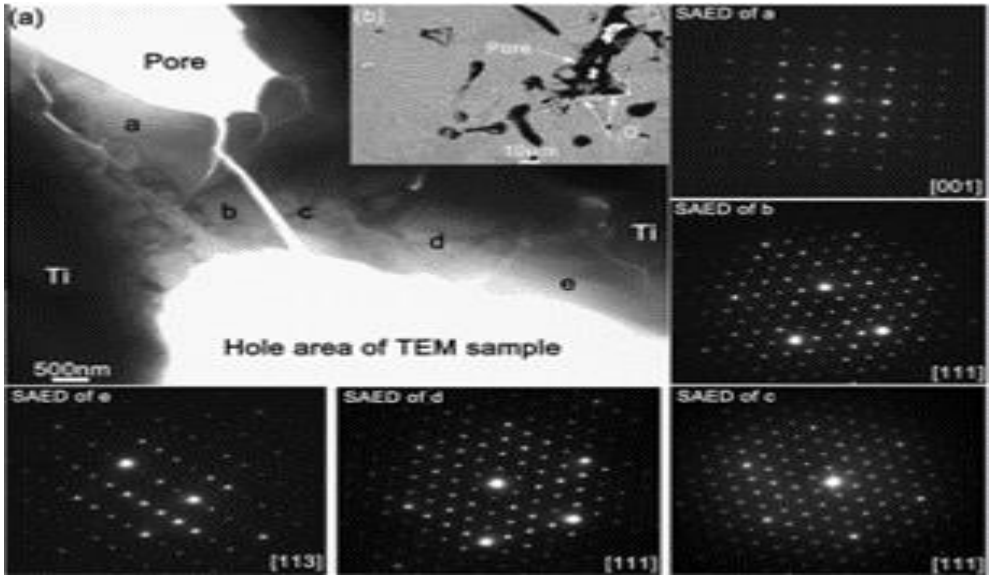

Figure 2. (a) Five phases of yttrium oxide in Ti-2.25Mo-1.5Fe alloys with the addition of YH_2 of TEM results and SAED patterns. (b) The place of yttrium oxide in as-sintered microstructures of back-scattered SEM[16]

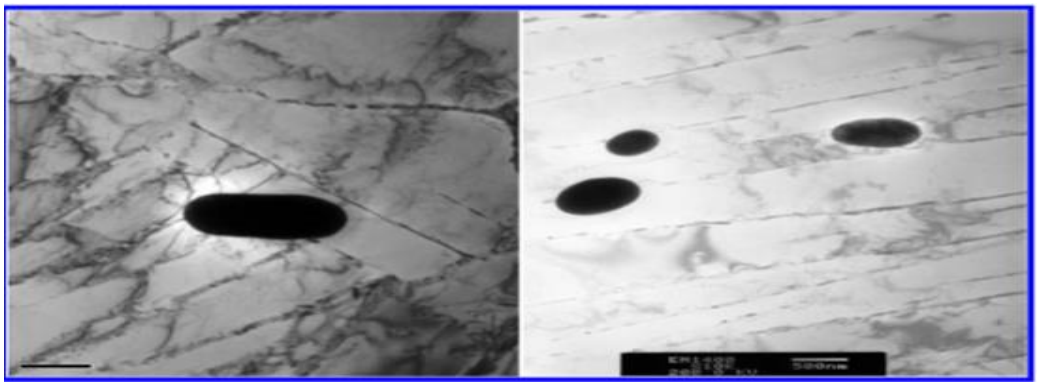

Figure 3. TEM of yttrium oxide particles in fatigue samples of Ti-6Al-2.75Sn-4Zr-0.4Mo-0.45Si-0.1Y (wt.%) at 500 MPa (R = 0.1) for $9.527x10^5$ cycles. No fatigue cracks found in yttrium oxide particles[16]

TEM was applied in the as-sintered alloy of Ti-2.25Mo-1.5Fe-0.6Y, and as a result, no Ti-Y phase was detected. The small Y solubility in Matrix Ti is proven from TEM-EDX. This result is in accordance with phase diagram Ti-Y where the yttrium oxide phase free of other elements is observed. Yan and Liu[16] stated that five phases of binary yttrium oxide had been observed on as-sintered Ti-2.25Mo-1.5Fe-0.6Y alloys with a SAED and SEM back-scattered pattern of TEM. Big particulate yttrium oxide in fatigue microstructure can also be analyzed using TEM. In the produced RE oxide particles, no fatigue cracks are found.

Cerium Silicide

Scavenging oxygen can also be done by adding $CeSi_2$ compounds which are used to add Ce to PM Ti alloys. Refinement of microstructure, increased density, and increased sintered elongation resulted from the addition of ≤ 0.5 wt.% $CeSi_2$ to CP-Ti, Ti-10V-2Fe-3Al, and Ti-6Al-4V. The formation of CeO_2 and CeClxOy results from the addition of $CeSi_2$ to CP-Ti, Ti-10V-2Fe-3Al, and Ti-6Al-4V to 1 wt.%. Si transfers the solid solution into the matrix of titanium. During sintering, the cerium scavenges oxygen and chlorine from the titanium matrix. Stable particles of the CeO_2 and CeClxOy effectively inhibit β-Ti grain growth. These particles form along or near the boundaries of the grain and are responsible for microstructural refinement. A slight increase in sintered density, with $CeSi_2$ ≤ 0.5 wt.%. For the addition of > 0.5 wt.%, $CeSi_2$ contributes to a reduction in the sintered density because the effect of Si material on the sintering densification is preferred.

The optimal addition, according to Yang and Luo[26] is 0.5 wt.% $CeSi_2$ above that the elongation decreases due to reduced sintered density and coarse particulate formation CeO_2.

Use of Oxygen Scavenger Based on Oxygen-Stabilized Compounds

Besides RE-based materials, Yan and Tang[13] stated that oxygen scavenging was also carried out with the following oxygen-stabilized compounds.

Ti_2C type compounds

The formation of Ti_2C compound:

a. The formation of Ti_2C is related to oxygen and forms the oxygen stabilizer of Ti_2C. The development of oxygen-sensitive stages such as grain boundaries α, α, and/or α_2 could be prevented as a consequence of the decreased local concentration of oxygen.
b. Oxygen solubility in Ti_2C is generally lower than 10%, suggesting that Ti_2C's oxygen-scavenging potential is weaker than RE-based materials such as YH_2, resulting in Y_2O_3 forming containing up to 60 % Oxygen.
c. Scavenging oxygen by Ti_2C formation appears dependent on the alloy. A Ti_2C phase, for example, can be formed in a Ti-15Ta alloy but has little oxygen around the Ti matrix. This is because the Ti matrix's broad lattice parameter adds element Ta, which increases the propensity for oxygen to occupy the interstitial void in the Ti matrix compared to the Ti_2C step.
d. There is still confusion. For instance, Ti_2C contained oxygen more than the Ti matrix in the Ti-15Mo PM test. It should be remembered that it is hard to quantify light elements such as carbon and oxygen and perhaps this is why these variations occur.

Table 1. The concentration of oxygen in Ti alloys containing carbon[13]

Ti alloy	Overall carbon content (wt.%)	Ti-C phase	Carbon concentration in Ti-C phase	Oxygen concentration in Ti-C phase	Ref.
Ti-15-3 (Ti-15V-3Al-3Sn-3Cr)	0.2-0.7	Ti_2C or Ti(CO)	0.5 in C/Ti ratio	Higher than matrix	29
Ti-15Mo (PM)	0.032	Ti_2C	0.54 in C/Ti	Higher than matrix	30
Ti-13Cr	0.15	Ti_2C	-	-	31
Ti-15Cr	0,2	Ti_2C	0.56 in C/Ti ratio	Higher than matrix	31
Ti-15Ni	0.2	Ti_2C	0.98	Higher than matrix	31
Ti-15Mo	0.2	Ti_2C	0.5	Lower than matrix	31

$Ti_4Fe_2O_x$ type compounds

The second type of compound that is oxygen-stabilized is the intermetallics group[13], abbreviated with Ti_2MO_x (M = Fe, Co, Ni; x values up to 0.5) or $Ti_4M_2O_y$ (M = Fe, Co, Ni). This is the electronic concentration phase (e/a). $Ti_4Fe_2O_x$ is an example, may form the intermetallic process with the presence of TiFe even with oxygen concentrations in trace levels (about 0.1 at% ≈ 0.03 wt.%). The secret to the formation of $Ti_4Fe_2O_x$ is seen by the presence of TiFe in the microstructure, but it usually is not formed in PM Ti materials because Fe is a potential β stabilizer that appears to remain in the β-Ti phase. In other words, other studies of the $Ti_4Fe_2O_x$ phase in PM Ti material expect that this intermetallic phase could be available in PM Ti to be able to scavenge oxygen from PM Ti. The mechanism is unclear. All in all, however, oxygen-scavenging, the efficacy of this compound is expected to be greater than Ti_2C.

Finally, it should be noted that the shape of material RE oxides, oxygen stabilizers Ti_2C, or $Ti_4Fe_2O_x$ can increase the ductility of PM Ti as-sintered materials. Size and distribution must be controlled.

Protection and Regulation of Sintering Atmospheric

The atmosphere during sintering can be protected and regulated by the use of inert gases such as Argon, N_2, H_2, and vacuum. In his research, Suleiman Ahmad et al.[18] stated that at high temperatures, Ti-6Al-4V would react to form titanium dioxide (TiO_2) with oxygen which gives problems during sintering and then affects the mechanical and microstructural properties. This response can maybe prevent either by using argon gas or under vacuum. During sintering, the bound part will be heated so that the powder is densified by reducing pores. It is supposed that the gas impurities in argon have a strong influence in terms of densification and properties.

Samples from the PE/PS formulation with argon were added to the sintering atmosphere. The experimental density of 4.375 g/cm^3 of tensile strength was stated at 1000.100 MPa in comparison with samples in vacuum conditions which did not show a substantial increase with a density of 3.943 g/cm^3 and tensile strength at 325.976 MPa. PE/PW/SA samples from vacuum also showed no enhanced properties of sintered. However, with the addition of argon flow, the density can reach 4.359g/cm^3 and the tensile strength of 940.823MPa. Sintered Ti alloys with argon show improved densification compared to vacuum with higher strength, improved elongation, and decreased porosity. In argon, particles of powder are connected, indicating densification is obtained due to the non-reactive nature of the inert gas, which prevents undesirable chemical reactions.

Table 2. Sintering Conditions Ti-6Al-4V[18]

Sintering condition	Sintering temperature (1100 ^{0}C)			
	Vac. Atmosphere		Ar. Atmosphere	
Formulation	PE/PS	PE/PW/PS	PE/PS	PE/PW/SA
Sample	Sample A	Sample B	Sample C	Sample D

Table 3. Physical and mechanical properties of as-sintered Ti-6A-4V[18]

Sample	Density (g/cm^3)	Porosity (%)	Tensile strength (MPa)	Elongation (%)	Shrinkage
Sample A	3.943	12.39	325.976	0.72	16.33
Sample B	4.341	3.52	494.079	0.30	15.72
Sample C	4.375	2.78	1000.10	0.73	15.18
Sample D	4.359	3.13	940.823	0.73	14.69

In the Banerjee and Joens[32] study, titanium alloys were processed with powder metallurgy (PM) sintered in a vacuum, the higher, the better. This philosophy is carried out on Ti-MIM alloys. In the MIM process, most of the gas binder exists, which affects the vacuum level therefore the interstitial element is taken from titanium. MIM-Ti 6-4 is processed in MIM furnaces, the best results are obtained using argon flow. By using argon, the highest elongation is obtained, and the oxygen content is lower.

Table 4. Sintering Conditions with Argon and Vacuum[32]

Sinter run	Atmosphere	Density (g/cm^3)	TS in MPA (ksi)	0.2% YS in MPA (ksi)	% Elong.	% N	% C	% O
1-121313	Argon	4.23	889 (129)	753 (109)	5.6	0.028	0.11	0.21
1-121613	Ar-HiVac	4.24	922 (134)	784 (114)	4.6	0.029	0.15	0.25
1-121713	HiVac	4.24	910 (132)	812 (118)	3.3	0.028	0.16	0.28
1-121813	HiVc ND	4.23	931 (135)	804 (117)	3.3	0.029	0.17	0.32

In the Heaney and German studies[33] which used vacuum and argon atmospheres, it was found that the vacuum atmosphere consistently provided higher oxygen content than in argon.

Table 5. Oxygen levels at 1300 ^{0}C as-sintered Ti powder[33]

Powder	Oxygen level in a vacuum (wt.%)	Oxygen level in argon (wt.%)
A – TSP350	4280	3030
B – Tilop 150H	3530	3270
C – Tilop 45	1770	1370

Hidalgo and Ebel[34] researched the impact of oxygen on mechanical properties and the microstructure of titanium alloys. The effect of impurities on the microstructure, ductility, and fatigue resistance of refined alloys Ti-6Al-

7Nb by metal injection molding is carried out. The first study of the impact of oxygen content on crack initiation and propagation was carried out with microstructure observation and fractured applications using light and electron microscopy (SEM).

Table 6. The content of interstitial elements in samples with a temperature of 400 ^{0}C[34]

Treatment time [min]	O-content [wt.%]	N-content [wt.%]	C-content [wt.%]
As sintered	0.22	0.01	0.03
3	0.38	0.03	0.04
10	0.41	0.02	0.04
30	0.43	0.02	0.04
60	0.44	0.02	0.04
900	0.60	0.03	0.04

Table 7. Tensile parameters of the sample at different oxygen contents[34]

O-content [wt.%]	Tensile strength [MPa]	Yield strength [MPa]	Plastic elongation [%]	Young modulus [GPa]
0.22	795	692	16	100
0.38	876	759	16	92
0.41	886	775	12	95
0.43	893	783	11	101
0.44	898	788	10	99
0.60	925	823	3	100

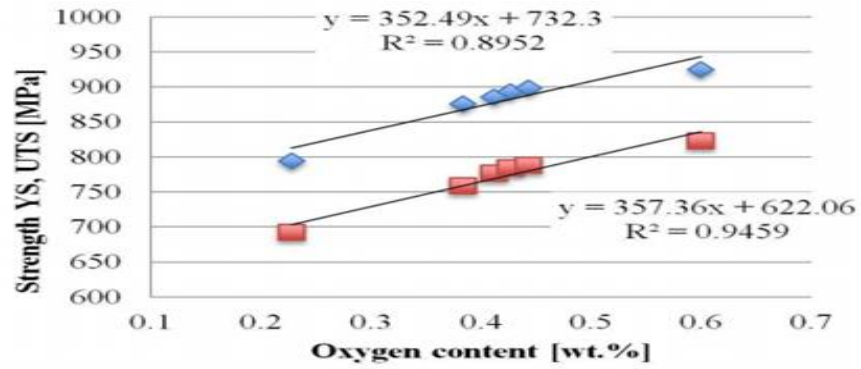

Figure 4. Effect of oxygen on tensile strength and yield strength of MIM Ti-6-Al-7Nb[34]

Good ductility is shown in as-sintered samples as a result of the lowest impurity content. The fracture surface shows most of the dimple rupture characteristics of ductile MIM material.

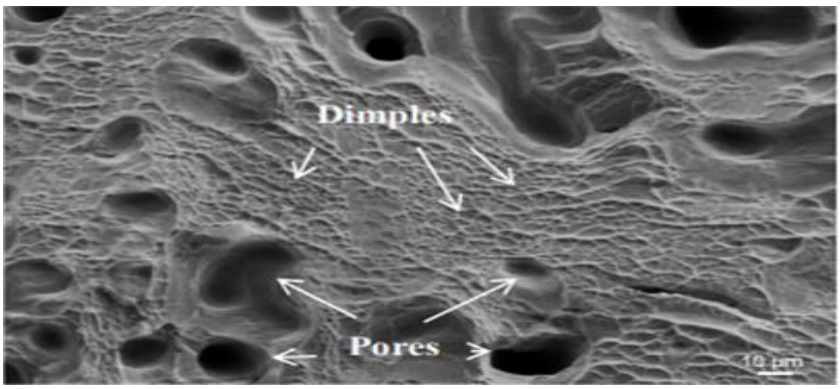

Figure 5. Fracture ductile with the appearance of dimples in as sintered samples[34]

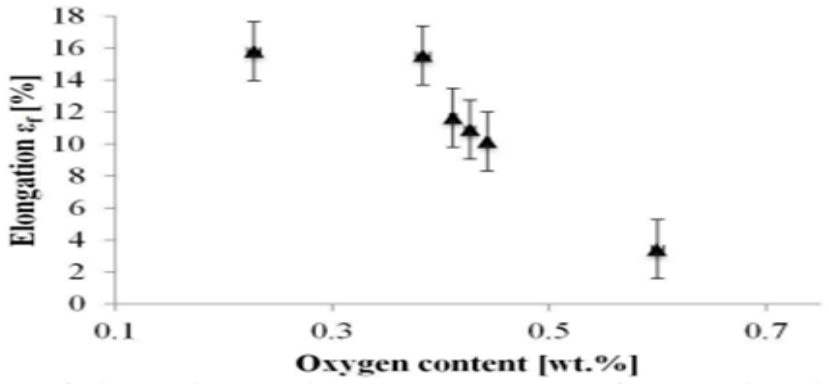

Figure 6. Dependence of elongation on oxygen content from MIM Ti-6Al-Nb samples[34]

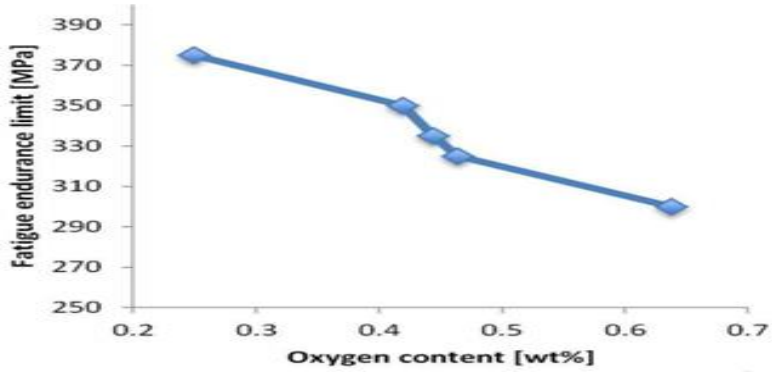

Figure 7. Effect of oxygen content on fatigue endurance limit (10^7 cycles) of MIM Ti-6Al-7Nb[34]

Ductility drops significantly when the oxygen content reaches 0.38 wt.%. Above this value, areas with transgranular brittle fractures are characterized by facets on fracture surfaces.

In the research of Budin and Jaafar[35], the effect of different sintering atmospheres and sintering temperatures was carried out to see the mechanical properties of WC-Co composites.

a. 95% nitrogen (N_2) gas mixed with 5% hydrogen (H_2) gas is used as the sintering atmosphere in the tube furnace.
b. The vacuum atmosphere is used in vacuum furnaces.

Sintering temperature was carried out at 1300 ^{0}C and 1400 ^{0}C. Relatively higher density, hardness, and transverse rupture strength (TRS) in sintered parts were observed. Sintering under the N_2-H_2 atmosphere shows better mechanical properties. Low mechanical properties are observed in a vacuum atmosphere due to over-sintering, which leads to grain growth and phase formation η. The results prove that relative density, hardness, and TRS increase due to higher sintering temperatures. High temperatures increase the densification process and effectively reduce pores. In sections sintered in the N_2-H_2 atmosphere, a higher relative density, hardness, and TRS were observed at the same time. Low mechanical properties are shown in parts sintered in a vacuum atmosphere due to over-sintering. Over-sintering leads to grain growth activity and phase formation η, which results in a fragile WC-Co composite.

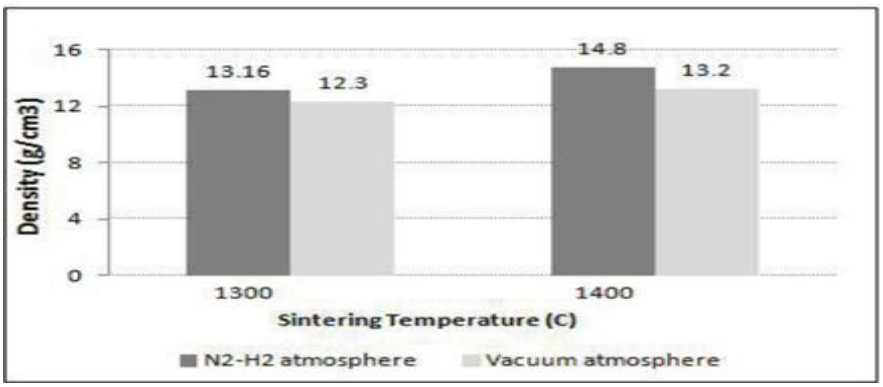

Figure 8. Comparison of Relative Density at sintering temperatures of 1300 ^{0}C and 1400 ^{0}C [35]

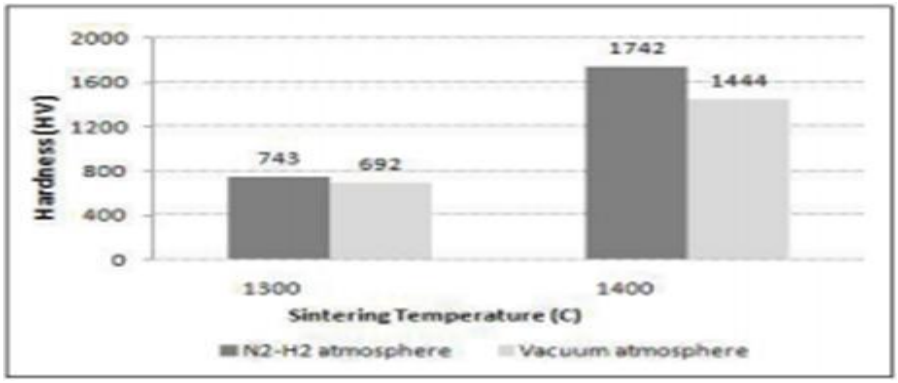

Figure 9. Comparison of Hardness at sintering temperatures of 1300 ^{0}C and 1400 ^{0}C [35]

Research by Padmavathi et al.[36] on Al-1Mg-0.8Si-0.25Cu (6711) and Al-7Zn-2.5Mg-1Cu (7775) alloys shows the effect on microstructure, densification, properties, and phase analysis of the atmospheric sintering and heating modes. Impact of sintering atmosphere and heating mode on the alloys Al-1Mg-0.8Si-0.25Cu (6711) and Al-7Zn-2.5Mg-1Cu (7775) densification, microstructure, phase analysis, and properties. The compact is heated to 630 ^{o}C with a conventional furnace and 2.45 GHz microwave oven under vacuum, N_2, Ar, and H_2.

Table 8. The impact of heating mode and sintering atmosphere on response to densification sintered at 630 ^{0}C [36]

Sintering atmosphere	Sintered density/%Th	
Heating mode/alloy composition	6711	7775
Vacuum (CON)	96.8	91.8
Vacuum (MW)	97.5	...
Nitrogen (CON)	96.1	91.6
Nitrogen (MW)	94.2	85.8
Argon (CON)	94.7	88.6
Argon (MW)	93.4	88.0
Hydrogen (CON)	92.9	86.6
Hydrogen (MW)	92.4	77.4

*CON: conventional, MW: microwave

Table 9. The impact of the sintering atmosphere on the nature of transverse rupture strength and tensile sintered in conventional furnaces[36]

Sintering atmosphere/alloy composition	Transverse rupture strength/MPa	Yield strength/MPa	Ultimate tensile strength/MPa	Ductility/%
6711				
Vacuum	276	100	115	19
Nitrogen	237	83	103	23
Argon	228	50	89	13
Hydrogen	157	27	65	8.4
7775				
Nitrogen	146	101	120	6.4
Hydrogen	124	32	47	0.3

Both alloys compact within the microwaves and heat quickly (approximately 22 ^{0}C/min). The processing time by microwave sintering is reduced by about 55-58 %. The microwave sintering leads to greater alloy densification 6711 under vacuum followed by N_2. In comparison to traditional sintering, the 7775 alloy exhibits low densification in all atmospheres. Microwave sintering creates non-homogenous microstructures without/with a small amount of inter-metal steps for all compositions and atmospheres. This relates to less time available for diffusion into the Al matrix of alloying elements. Depending on the heating mode and environment, the conductivity, hardness and corrosion properties of both compacts are rising.

Table 10. The impact of atmospheric sintering and heating mode on parameters of corrosion in conventional furnaces and microwaves[36]

Heating mode	Sintering atmosphere	E_{corr}/mV	i_{corr}/µA cm ^{2}	Corrosion rate/x10^{-3} mmpy
Conventional	Vacuum	-766	0.478	0.23
	N_2	-693	0.154	0.18
	Ar	-845	2.040	22.32
	H_2	-935	4.350	45.78

Microwave	Vacuum	-1230	7.540	82.57
	N_2	-874	0.083	0.91

Arc Plasma Sintering

The use of Arc Plasma Sintering is a breakthrough to avoid the formation of TiO_2 because the sintering time is done in a short time ranged between 2-10 minutes. The variety of sintering time is required to get optimum sintering time. Silalahi et al.[37] conduct the study of the MgZn biomaterials using plasma heat in the Arc Plasma Sintering (APS). Samples with APS show high homogeneity with a smaller grid parameter compared to samples that are sintered with the conventional furnace. This is equal to the high solubility of Zn in the Mg matrix that is processed with APS. Added 6 wt .% Zn was forming MgZn alloy in solid solution with smaller crystal field distance. The manufacture of MgZn biomaterials produces good performance after sintering with APS, i.e. shorter time and lower energy. APS can be controlled with very low energy of 12 watts. In Silalahi research, et al.[37] the Arc Plasma Sintering (APS) is performed using argon gas to avoid oxidation. APS is operated at 12 volts and 1 ampere within 30 seconds. Sintering results compared to conventional furnaces; sintering is done at 350 ^{0}C for an hour.

In the research[38], Bandriyana et al. expressed sintering with a conventional furnace requiring high energy and long time. Meanwhile, APS is recognized as a good alternative to solidification of powder material such as the alloy Fe-25CR-Y_2O_3 because of its simple, low power consumption, and flexibility in the form of a specimen. APS uses plasma produced by the Argon gas dissociation, which is an exothermic process that produces temperatures of up to 2,000 ^{0}C. Plasma with easy-to-control diameter that allows for high-speed processes. The consolidation of samples of Fe-25Cr-Y_2O_3 is sintered with APS much faster compared to conventional furnaces.

In research on Sitompul et al.[39], Mg6Zn-xHAp biocomposite has been successfully synthesised using APS technology. The corrosion test shows that the higher the HAp in the material, the greater the corrosion rate in the NaCl solution. In this study, APS operated at a voltage of 12 volts and a current of 1 ampere for 30 seconds. APS Technology is sintering technology that utilizes argon gas plasma ionization between anode and cathode with impulse current. One of the strengths of APS is low energy consumption and a fast sintering process. The use of argon as a plasma manufacturer makes the material synthesised protected from the oxidation process occurring during sintering. This is a major consideration in selecting APS for use in the manufacture of biomaterials.

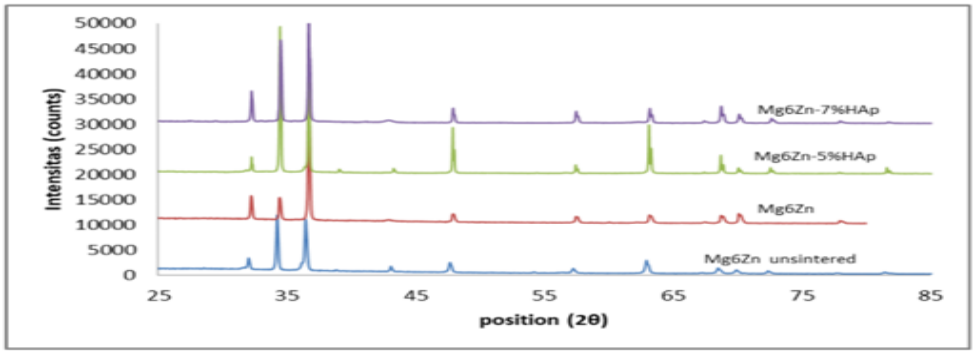

Figure 10. Hasil XRD[39]

The results of XRD (Figure 10) indicate that some Zn atoms have dissolved in Mg and form a solid solution characterized by a shift in the peak direction. This identifies that the biocomposite has a smaller distance between the crystal plane after the sintering process.

In the research of Wahyudi et al.[40] used SUP9 material, the pearlite carbon steel samples were sintered with APS for 1 second and 3 seconds at 1300-1500 ^{0}C. Hardness, depth of hardening and microstructure are carried out with Vickers and SEM-EDX microhardness tests.

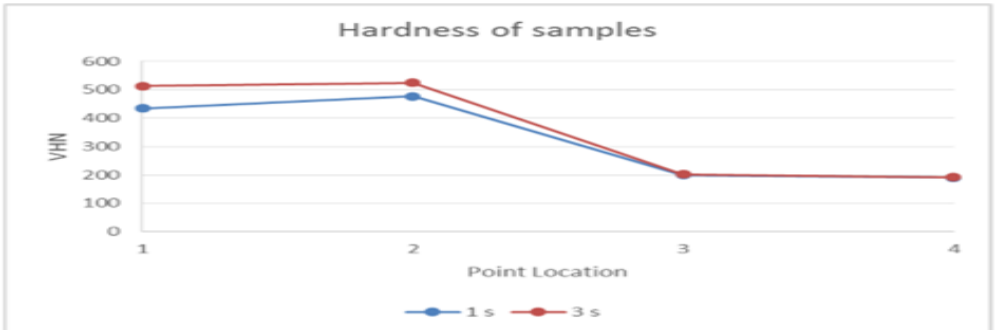

Figure 11. Hardness test of a sample[40]

Results showed that mechanical properties (Figure 11) were significantly improved with the formation of a single martensite structure as identified by Scanning Electron Microscopy (SEM). Surface hardness shows significant improvement almost three times of 190 VHN to 524 VHN after treatment. Furthermore, Energy Dispersive X-Ray Spectroscopy (EDX) results that the formation of a martensite layer that occurs without altering the

composition of the material. APS produces a uniform layer of hardness up to 250 µm. Research shows that the arc plasma sintering process manages to improve the mechanical properties of the steel in a short sintering time. In the research, Sugeng et al.[41] performed the synthesis of Zirconia-ODS (Oxide Dispersion Strengthen) with powder metallurgy with 3, 5, and 7 hour milling time, 20 tons static compression and sintering process with APS for 4 minutes. The synthesis produces a solid and tiny porous ODS steel samples. The longer the milling process will result in a more refined and predictable powder size it will refine the grain size and strengthen the alloy. The results obtained the higher the milling time is increasingly homogeneous phase Fe-Cr, improving the improvement of grain structures and increasing the hardness of alloys.

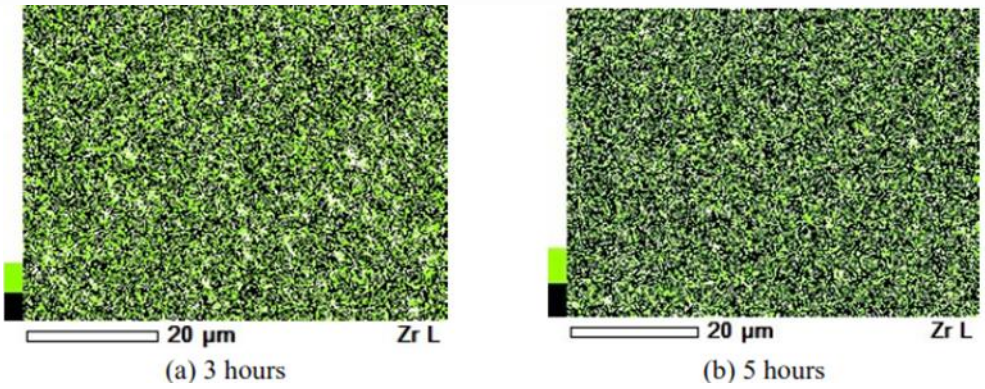

Figure 12. Mapped area Zr in alloy ODS-20Cr-0.5 ZrO2 with 3 hours and 5 hours milling time[41]

Based on the content of Zr observed in Figure 12, Zr is alloyed homogeneously and a predictable increase in milling time affects zirconia disperse homogenisation to enhance the properties of the ODS alloy.

In the study of Silalahi et al.[37], the microstructure and deformation of superalloy 57Fe17Cr25NiSi were studied. A superalloy is manufactured from a mixture of Ferro-granular scrap, Ferrochrome, Ferro Silicon and Ferro Manganese with casting method and in-sintering with APS for 4 minutes and 8 minutes. Superalloy has been proposed in a nuclear power plant on XRD results obtained shift in value 2 (in the greater direction with increasing the time of sintering with APS (Table 11). Table 12 shows the increasing sintering time with APS, the smaller the spacing between fields.

Table 11. Results of gaussian regression fittings with 57Fe-17Cr-25Ni-Si superalloy XRD peak[37]

(hkl)	As-cast			4-minute APS			8-minute APS		
	$2\theta_0$	FWHM/β (°)	I_0	$2\theta_0$	FWHM/β (°)	I_0	$2\theta_0$	FWHM/β (°)	I_0
(111)	43.64(5)	0.221(9)	1054	43.89(1)	0.109(2)	7344	43.702(1)	0.1026(2)	3364
(200)	50.75(4)	0.376(4)	214	50.899(9)	0.141(2)	938	74.875(1)	0.05966(1)	1446
(220)	74.71(5)	0.016(6)	91.82	74.82(1)	0.071(2)	938	74.875(1)	0.05966(1)	895
(311)	-	-	-	90.868(7)	0.095(1)	637	90.94(1)	0.10773(2)	1231
(222)	-	-	-	96.169(1)	0.12(2)	369	96.28(3)	0.1377(2)	212

Table 12. Distance value between fields, d_{hkl} for 57Fe-17Cr-25Ni-Si superalloy[37]

Sample	d_{111} (Å)	d_{200} (Å)	d_{220} (Å)	d_{311} (Å)	d_{222} (Å)
As-cast	2.072474	1.797427	1.269497	-	-
4-minute APS	2.070083	1.792515	1.267903	1.081165	1.035123
8-minute APS	2.069542	1.791825	1.267108	1.800496	1.034334

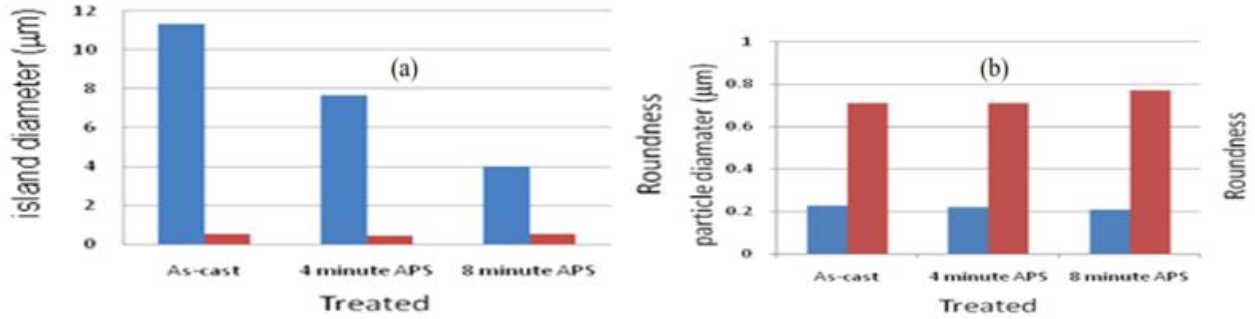

Figure 13. Carbide island histograms (blue) and carbide particles (red)[37]

The amount of eutectic structures on the inter-dendrite boundary decreases with the increased time of sintering. The sintering process (Fig. 13) leads to the improvement of the carbide island (Cr, $Fe)_{23}C_6$ in the eutectic structure and seems to not affect the development of particles (Cr, $Fe)_7C_3$ on the side of the dendrites matrix superalloy 57Fe-17Cr-25Ni-Si.

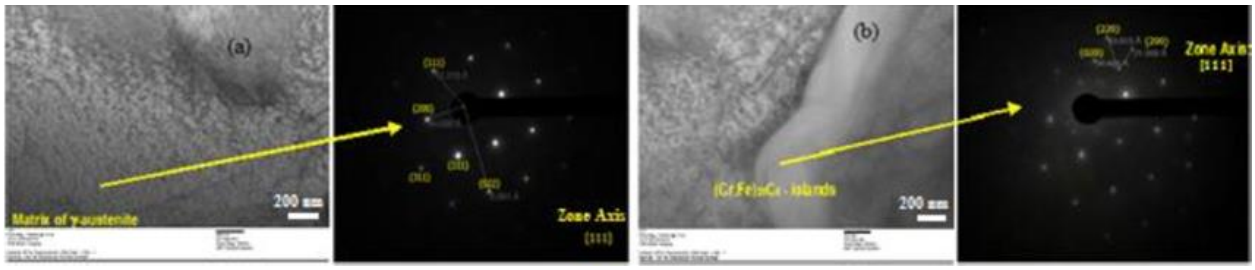

Figure 14. TEM and SAED from (a) matrix; (b) Island (Cr, Fe) 23C6 in 57Fe-17Cr-25Ni-Si superalloy austenite with 4 minutes APS[37]

Figure 14 shows a TEM and SAED image of the matrix area and super Alloy 57Fe-17Cr-25Ni-Si islands. The Island (Cr, $Fe)_{23}C_6$ is measured at 2100 x 600 nm. The SAED pattern of the matrix austenite shows the FCC zone axis pattern [111] as shown in Figure 14a, and island's SAED pattern (Cr, $Fe)_{23}C_6$ has the FCC pattern [001] as shown in Figure 14b. From SAED in Figure 14a, the distance between the fields, the d_{hkl} measured according to the d_{hkl} obtained from the XRD measurement for the sample sintering with APS for 4 minutes with the distance between fields measured for:

a. d_{111} (SAED) = 12.276 Å is about 6 times larger than the d_{111} (XRD) value measured bys the XRD = 2.070083 Å method.
b. d_{200} (SAED) = 14.088 Å is about 8 times greater than the value obtained by the XRD method of d_{200} (XD) = 1.792515 Å,
c. d_{220} (SAED) = 6.561 Å is about 5 times greater than the value gained from XRD d_{220} (XRD) measurement = 1.267903 Å

In his research[42], Bandriyana et al. developed an ODS alloy steel for a nuclear power plant that has good resistance to creep because of its microstructural uniqueness. Investigation of microscopy on the formation of microstructures during the alloying process, especially in the initial stage is conducted to study the correlation between the structure and properties of ODS. This makes it possible thanks to APS sintering devices that can stimulate time-dependent alloy processes. The ODS samples themselves were synthesized with a composition of 88 wt.% Fe and 12 wt.% Cr was dispersed with 1 wt.% ZrO_2 in the form of a nanopowder mixed in high-power isostatic compressed energy to form a sample of coins and then sintering with APS.

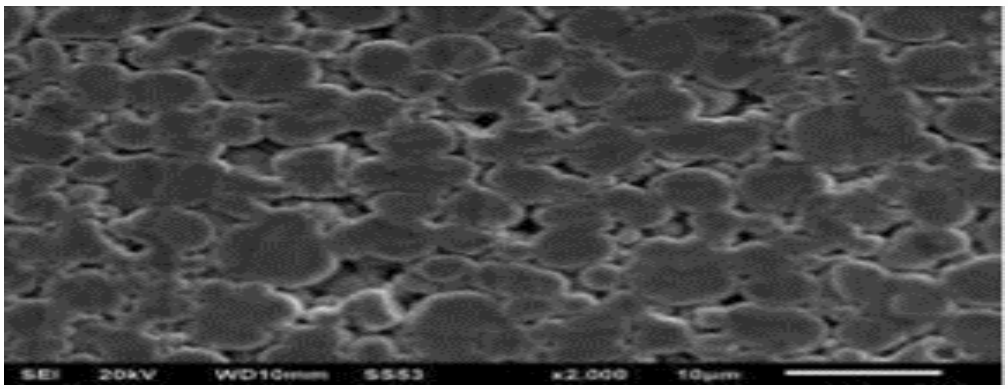

Figure 15. SEM from the sample after 20 tons of compression[42]

Figure 15 shows a single Fe and Cr particle. The result of the pressing process is good enough that results in porosity less than 15%.

CONCLUSION

In the MIM process, at high temperatures, Ti-6Al-4V will react with oxygen to form titanium dioxide (TiO_2) which causes problems during sintering thereby affecting the microstructure and lowering the mechanical properties of the alloy Ti-6Al-4V. Some studies have made efforts to minimize the formation of TiO_2 with (a) the addition of the oxygen scavenger of rare earth and (b) the addition of oxygen scavenger from a compound that is oxygenated, as well as the control and regulation of sintering atmospheres. Sintered Ti alloys with argon atmosphere showed improved densification compared to vacuum atmosphere as well as higher tensile strength, improved elongation and decreased porosity. While study of effect sintering temperature on mixture atmosphere of N_2-H_2 atmosphere showed improved on hardness and strength on higher temperature. It also had better result if compare with vacuum atmosphere. In the process of sintering, the use of Arc Plasma Sintering (APS) is a breakthrough to avoid the formation of TiO_2 because the time of sintering is done in a short time ranging from 2-10 minutes. On making of MgZn biomaterials with APS show high homogeneity with a smaller grid parameter compared to samples that are sintered with the conventional furnace. The manufacturing process also shown better performance with lower energy and shorter sintering time. Hence the more efficient of Ti-6Al-4V manufacture would be achieved by optimizing combination of oxygen scavenger from RE metals with controlled atmosphere on higher sintering temperature by using APS.

ACKNOWLEDGMENTS

This research was financially supported by Directorate Research and Community Service, University of Indonesia through PUTI Doctor No. NKB-681/UN2.RST/HKP.05.00/2020.

REFERENCES

1. Lee, J. H., Kwon, J. S., Moon, S. K., Uhm, S. H., Choi, B. H., Joo, U. H., ... & Kim, K. N. (2016). Titanium-silver alloy miniplates for mandibular fixation: In vitro and in vivo study. *Journal of Oral and Maxillofacial Surgery*, *74*(8), 1622-e1.
2. Ratner, B. D. (2015). The biocompatibility of implant materials. In *Host Response to Biomaterials* (pp. 37-51). Academic Press.
3. Rokosz, K., Hryniewicz, T., and Raaen, S. (2016). Development of plasma electrolytic oxidation for improved Ti6Al4V biomaterial surface properties. *The International Journal of Advanced Manufacturing Technology*, *85*(9-12), 2425-2437.
4. Dehghan-Manshadi, A., Bermingham, M. J., Dargusch, M. S., StJohn, D. H., and Qian, M. (2017). Metal injection moulding of titanium and titanium alloys: Challenges and recent development. *Powder Technology*, *319*, 289-301.
5. Bermingham, M. J., McDonald, S. D., & Dargusch, M. S. (2018). Effect of trace lanthanum hexaboride and boron additions on microstructure, tensile properties and anisotropy of Ti-6Al-4V produced by additive manufacturing. *Materials Science and Engineering: A*, *719*, 1-11.6.
6. Limberg, W., Ebel, T., and Kainer, K. U. (2013). Powder Injection Moulding Materials 2: Addition of Rare Earth Elements to MIM-processed Ti-6Al-4V. In *European Congress and Exhibition on Powder Metallurgy. European PM Conference Proceedings* (p. 1). The European Powder Metallurgy Association.
7. Froes, F. H. S., and Qian, M. (2015). A perspective on the future of titanium powder metallurgy. In *Titanium Powder Metallurgy* (pp. 601-608). Butterworth-Heinemann.
8. Jurisch, M., Studnitzky, T., Andersen, O., and Kieback, B. (2016). Thermohydrogen processing of 3D screen printed titanium parts. In *Key Engineering Materials* (Vol. 704, pp. 251-259). Trans Tech Publications Ltd.
9. Holm, M., Ebel, T., and Dahms, M. (2013). Investigations on Ti–6Al–4V with gadolinium addition fabricated by metal injection moulding. *Materials & Design*, *51*, 943-948.
10. Limberg, W., Pyczak, F., and Ebel, T. (2016). Colony Refinement of MIM-processed Ti-6Al-4V by Addition of Different Yttrium Compounds. In *European Congress and Exhibition on Powder Metallurgy. European PM Conference Proceedings* (pp. 1-7). The European Powder Metallurgy Association.
11. Thompson, G. E., Skeldon, P., Zhou, X., Shimizu, K., Habazaki, H., and Smith, C. J. E. (2003). Improving the performance of aerospace alloys. *Aircraft Engineering and Aerospace Technology*.
12. Okabe, T. H., Hirota, K., Kasai, E., Saito, F., Waseda, Y., and Jacob, K. T. (1998). Thermodynamic properties of oxygen in RE–O (RE= Gd, Tb, Dy, Er) solid solutions. *Journal of alloys and compounds*, *279*(2), 184-191.
13. Yan, M., Tang, H. P., and Qian, M. (2015). Scavenging of oxygen and chlorine from powder metallurgy (PM) titanium and titanium alloys. In *Titanium powder metallurgy* (pp. 253-276). Butterworth-Heinemann.
14. Hidalgo, A. A., Limberg, W., Ebel, T., Frykholm, R., Carreño-Morelli, E., and Pyczak, F. (2018). Influence of alloying elements in fatigue properties of α/β titanium alloys. In *Key Engineering Materials* (Vol. 770, pp. 80-86). Trans Tech Publications Ltd.
15. Yan, M., Liu, Y., Schaffer, G. B., and Qian, M. (2013). In situ synchrotron radiation to understand the pathways for the scavenging of oxygen in commercially pure Ti and Ti–6Al–4V by yttrium hydride. *Scripta Materialia*, *68*(1), 63-66.
16. Yan, M., Liu, Y., Liu, Y. B., Kong, C., Schaffer, G. B., and Qian, M. (2012). Simultaneous gettering of oxygen and chlorine and homogenization of the β phase by rare earth hydride additions to a powder metallurgy Ti–2.25 Mo–1.5 Fe alloy. *Scripta Materialia*, *67*(5), 491-494.
17. Yu, C. (2014). *Ti powder sintering: impurity, sintering atmosphere and alloy design* (Doctoral dissertation, ResearchSpace@ Auckland).
18. bin Suleiman Ahmad, M. J., bin Abdullah, A. N., Bin Ibrahim, R., Mohamad, M., Abu Kasim, N. B., Bin Dato'Abdul Kadir, M. R., ... and Shimizu, T. (2013). Effect of sintering conditions on mechanical properties and microstructure of Titanium alloy produced by metal injection moulding (MIM). In *Advanced Materials Research* (Vol. 686, pp. 164-169). Trans Tech Publications Ltd.

19. Limberg, W., and Ebel, T. (2016). Metal Injection Moulding of Ti-6Al-4V with Yttrium addition. In *Key Engineering Materials* (Vol. 704, pp. 20-27). Trans Tech Publications Ltd.
20. Leyens, C., and Peters, M. (Eds.). (2003). *Titanium and titanium alloys: fundamentals and applications*. John Wiley & Sons.
21. Lütjering, G., and Williams, J. C. (2007). *Titanium*. Springer Science & Business Media.
22. Gigliotti, M. F. X., and Woodfield, A. P. (1993). The roles of rare earth dispersoids and process. *Metallurgical Transactions A*, *24*(8), 1761-1771.
23. Sastry, S. M. L., Meschter, P. J., and O'neal, J. E. (1984). Structure and properties of rapidly solidified dispersion-strengthened titanium alloys: Part I. Characterization of dispersoid distribution, structure, and chemistry. *Metallurgical Transactions A*, *15*(7), 1451-1463.
24. De Castro, V., Leguey, T., Monge, M. A., Munoz, A., Pareja, R., Amador, D. R., ... and Victoria, M. (2003). Mechanical dispersion of Y2O3 nanoparticles in steel EUROFER 97: process and optimisation. *Journal of nuclear materials*, *322*(2-3), 228-234.
25. Bilobrov, I., and Trachevsky, V. (2011). Approach to modify the properties of titanium alloys for use in nuclear industry. *Journal of nuclear materials*, *415*(2), 222-225.
26. Yang, Y. F., Luo, S. D., Schaffer, G. B., and Qian, M. (2013). Impurity scavenging, microstructural refinement and mechanical properties of powder metallurgy titanium and titanium alloys by a small addition of cerium silicide. *Materials Science and Engineering: A*, *573*, 166-174.
27. Liu, Y., Chen, L., Wei, W., Tang, H., Liu, B., and Huang, B. (2006). Improvement of ductility of powder metallurgy titanium alloys by addition of rare earth element. *JOURNAL OF MATERIALS SCIENCE & TECHNOLOGY*, *22*(4), 465-469.
28. Ramaswamy, R., Selvam, B., Marimuthu, P., and Elango, N. (2018). Investigation of densification behaviour on yttrium oxide reinforced Ti-6Al-4V nano-composite through powder metallurgy. *Int J Mech Prod Eng Res Dev*, *8*(2), 433-442.
29. Chen, Z. Q., and Loretto, M. H. (2004). Effect of carbon additions on microstructure and mechanical properties of Ti-15-3. *Materials science and technology*, *20*(3), 343-349.
30. Yan, M., Qian, M., Kong, C., and Dargusch, M. S. (2014). Impacts of trace carbon on the microstructure of as-sintered biomedical Ti–15Mo alloy and reassessment of the maximum carbon limit. *Acta biomaterialia*, *10*(2), 1014-1023.
31. Chu, M., Jones, I. P., and Wu, X. (2005). Effect of carbon on microstructure and mechanical properties of a eutectoid β titanium alloy. *Journal of materials engineering and performance*, *14*(6), 735-740.
32. Banerjee, S., & Joens, C. J. (2016). Sintering powder metal injection molded (MIM) titanium alloys: in vacuum or argon?. In *Key Engineering Materials* (Vol. 704, pp. 113-117). Trans Tech Publications Ltd.
33. Heaney, D. F., and German, R. M. (2004). PM Lightweight and Porous Materials: Advances in the Sintering of Titanium Powders. In *European Congress and Exhibition on Powder Metallurgy. European PM Conference Proceedings* (Vol. 4, p. 1). The European Powder Metallurgy Association.
34. Hidalgo, A. A., Ebel, T., Limberg, W., and Pyczak, F. (2016). Influence of oxygen on the fatigue behaviour of Ti-6Al-7Nb alloy. In *Key Engineering Materials* (Vol. 704, pp. 44-52). Trans Tech Publications Ltd.
35. Budin, S., Jaafar, T. R., and Selamat, M. A. (2017). Effect of Sintering Atmosphere on The Mechanical Properties of Sintered Tungsten Carbide. In *MATEC Web of Conferences* (Vol. 130, p. 03006). EDP Sciences.
36. Padmavathi, C., Upadhyaya, A., and Agrawal, D. (2011). Effect of atmosphere and heating mode on sintering of 6711 and 7775 alloys. *Materials Research Innovations*, *15*(4), 294-301.
37. Silalahi, M., Sitompul, H., Manalu, J. L., Dahlan, K., Noviana, D., and Dimyati, A. (2017). Novel Technology on Sinthesizing Mg-Zn Biomaterial Using Arc Plasma Sintering. *Asian Journal of Applied Sciences*, *5*(3).
38. Bandriyana, A. D., Sujatno, A., Salam, R., Sumaryo, P., and Untoro, B. S. (2018). Microstructures and Hardness of the High Chromium Oxide Dispersion Strengthened Alloy Fe-25Cr-Y2O3 Sintered by the Arc Plasma Sintering (APS). In *IOP Conference Series: Materials Science and Engineering* (Vol. 333, p. 012045).
39. Sitompul, H., Gunanto, Y. E., Izaak, M., Silalahi, M., and Dimyati, A. (2018, November). Synthesis of Mg6Zn-xHAp Biocomposites Using Arc Plasma Sintering. In *Journal of Physics: Conference Series* (Vol. 1120, No. 1, p. 012044). IOP Publishing.
40. Wahyudi, H., Dimyati, A., and Sebayang, D. (2018, March). Surface martensitization of Carbon steel using Arc Plasma Sintering. In *IOP Conf. Series: Materials Science and Engineering* (Vol. 343, p. 012032).
41. Sugeng, B., Bandriyana, B., Salam, R., Sujatno, A., & Dimyati, A. (2018, March). Microstructure and phase analysis of Zirconia-ODS (Oxide Dispersion Strengthen) alloy sintered by APS with milling time variation. In *IOP Conference Series: Materials Science and Engineering* (Vol. 343, No. 1, p. 012035). IOP Publishing.
42. Bandriyana, B., Sujatno, A., Salam, R., Dimyati, A., and Untoro, P. (2017, July). Microscopy of Alloy Formation on Arc Plasma Sintered Oxide Dispersion Strengthen (ODS) Steel. In *IOP Conference Series: Earth and Environmental Science* (Vol. 75, p. 012021).